PERFORMANCE OF CEMENT CLAY INTERLOCKING HOLLOW BRICK MASONRY WALLS SUBJECTED TO DIAGONAL COMPRESSION

PANUWAT JOYKLAD[1,*], QUDEER HUSSAIN[2]

[1]Department of Civil and Environmental Engineering,
Srinakharinwirot University, Thailand
[2]Construction and Maintenance Technology Research Center (CONTEC),
School of Civil Engineering and Technology, Sirindhorn International Institute
of Technology, Thammasat University, Pathumthani, Thailand
*Corresponding Author: panuwatj@g.swu.ac.th

Abstract

This study presents an experimental investigation on the diagonal compressive response of cement-clay interlocking (CCI) hollow brick masonry walls. The diagonal compressive responses of the masonry walls were investigated by performing laboratory tests on large size (1000×1000×125 mm) CCI hollow brick masonry walls. CCI hollow brick masonry walls were constructed using different techniques to represent existing construction practice in Thailand. A total of five masonry walls were constructed and tested under diagonal compression. One masonry wall was constructed by dry stacking of CCI hollow bricks over each other in the running bond pattern without using any binding material (i.e., un-grouted masonry wall). In the second and third walls, circular and square holes in the CCI bricks were filled with Ordinary Portland Cement (OPC)-Sand grout and high-performance non-shrink cement-sand grout, respectively. The remaining two walls (i.e., wall number 4 and 5) were similar to the wall number two and three, however, prior to the grout filling, steel bars were also inserted into the holes at different locations to reinforce the masonry walls. It was evidenced from the experimental results that cement grout impact, shear strength and shear modulus of the CCI brick masonry walls. It was also noticed that the reinforced CCI hollow brick masonry walls showed very ductile failure mechanism as compared with unreinforced masonry walls along with an increase in the ultimate diagonal load carrying capacity of the CCI masonry walls.

Keywords: Cement, Clay, Grout and masonry, Interlocking bricks, Shear Modulus, Shear strength.

1. Introduction

Masonry is one of the oldest building materials known to the man and is believed to have been in use for over 6000 years. Construction using masonry remains relatively popular in many parts of the world and is practiced widely even today. Masonry is composed of two different materials, namely: the masonry units and the mortar phase. Masonry units may be either solid or hollow and may be made of a wide variety of materials. Clay bricks, blocks of stone, concrete blocks, pressed earth bricks, calcium silicate bricks, soft mud bricks, etc. Are some examples of masonry units used in masonry construction [1].

Several experimental studies have been carried out on the compression behaviour of masonry under different load cases [2-9], including diagonal-compression, flexural test, uniaxial compression test, cyclic compressive loading, and so on [10]. The influence of mortar strength, thickness, material of bricks, and composite systems on the compressive failure were also investigated experimentally and theoretically [11-14]. Gurumo [15] performed diagonal compression tests on 1200×1200×250 mm adobe specimens adopting a reinforcement based on soil-cement bond beams with longitudinal pre-tensioning steel rods. Results indicated that the pre-stressed specimens carried almost twice the load of the un-reinforced adobe.

Sathiparan et al. [16] conducted diagonal compression tests on non-reinforced and polypropylene mesh reinforced adobe masonry wall specimens. The authors reported that the mesh effect was not observed before the wall crooked. After cracking, the mesh presence positively influenced the wall behaviour. San Bartolomé et al. [17] tested four small walls 800×800×180 mm under diagonal compression to evaluate the shear resistance. Tests were not effective as detachment occurred during the handling prior to the test, resulting in very low values for shear resistance, which are not cited in the publication.

Alecci et al. [18] investigated the shear strength of brick masonry walls assembled with different types of mortar. A comparison between the values of the masonry shear strength, calculated applying the three formulas available in the literature for the diagonal compression test data, and those obtained from laboratory tests on shear triplets was also performed. The strength values obtained by triplet tests are in good measure along the line of the results determined by diagonal tests and calculated by formulas.

Yardim and Lalaj [19] performed shear strengthening of un-reinforced masonry walls with different fiber reinforced mortar jacketing. The walls reinforced with ferrocement and polypropylene mortar, plaster exhibited a significant improvement in the shear strength capacity of up to 412% when compared to the control specimen.

The high demand of construction of buildings gives reason to find ways to fulfil and to solve the problems related to the construction. Interlocking brick system is an alternative system which is similar to the "LEGO blocks" that use less or minimum mortar to bind the bricks together. Interlocking bricks were introduced to reduce the use of manpower, hence fulfil the requirement of Industrialized Building System (IBS). Interlocking brick system is a fast and cost-effective construction system, which offers good solution in construction.

Nazar and Sinha [20, 21] investigated the behaviour of interlocking grouted stabilized sand-fly ash brick masonry under uniaxial cyclic compressive loading.

Five cases of loading at 0, 22.5, 45, 67.5, and 90° with the bed joints were considered. Results indicate that the load carrying capacity of interlocking grouted brick masonry is 63% of its unit strength of the specimens loaded perpendicular to bed joints, whereas the ultimate strength of a conventional masonry system varies from 30 to 40% of its unit strength.

Ronoh et al. [22] experimentally studied cement effects on the physical properties of expansive clay soil and the compressive strength of compressed interlocking clay blocks. The results indicate that the compressive strength of blocks increased with increase in cement content from 0% to 12% cement content. Out-of-plane structural responses of interlocking compressed earth block walls have also been investigated by Laursen et al. [23]. Bland [24] investigated the in-plane cyclic shear performance of interlocking compressed earth block walls. The interlocking compressed earth blocks (ICEBs) used in this experiment are dry stacked interlocking hollow units, which can be reinforced and grouted after they are laid. It was determined that the shear strength of fully grouted walls is significantly higher than that of partially grouted walls.

In Thailand, cement-clay interlocking (CCI) bricks made of locally available red clay are widely used to construct low-rise residential buildings throughout the country. These interlocking bricks are manufactured locally in small factories located in the different regions of Thailand. The CCI hollow bricks are usually used for the construction of load bearing and partition walls in three different ways. In the first method, the arrangement of the CCI bricks is such that they are placed on each other in the running bond pattern (without using any mortar and grout) to construct the masonry structures. In this pattern, the bonding strength is achieved by using interlocks. Mostly, this type of construction technique is used for load bearing walls in single-story residential buildings and boundary walls. In the second method, the construction of the masonry walls is similar to the first method with the only difference that holes in the CCI hollow bricks are filled with some kinds of cement-sand grouts to increase the bonding strength of the masonry wall. Whereas, in the third method, steel bars are also inserted into the holes to further enhance the bonding strength and lateral stability of the load bearing walls. The second and third type of construction technique is used for the construction of high-rise building (mostly 2-4 story building) and commercial facilities. In the past, a significant research has been undertaken to optimize the material properties of these CCI hollow bricks [25]. Namboonruang et al. [26], Yoosathaporn et al. [27], Namboonruang et al. [28], Joyklad [29] and Shakir and Mohammed [30] investigated the mechanical properties of these CCI hollow brick.

The CCI hollow brick masonry walls are main load carrying elements which can safely carry vertical loads without severe damages. However, the shear response of masonry walls is more complex and depends on the composite nature of interlocks, cement-sand grout and bricks. The determination of shear strength and shear modulus is very important for analytical predictions. Therefore, the primary objective of this research was to investigate the diagonal compressive response and deformability of CCI hollow brick masonry walls representing existing construction practices in Thailand. To achieve this goal an experimental program was developed and the diagonal compressive responses of the masonry walls were investigated by performing laboratory tests on large area (1000×1000×125 mm) CCI hollow brick masonry walls. CCI hollow brick

masonry walls were constructed using different techniques to represent existing construction practice in Thailand.

The scope of the research was limited to the diagonal compression loading of CCI hollow brick masonry walls under static loading. The size of the CCI brick masonry walls was designed according the available lab facilities such as the size and the capacity of the loading frame. CCI hollow bricks were collected from the local manufacturer in Thailand. The experimental results in terms of ultimate load carrying capacity, diagonal compression and failure modes are briefly discussed and presented in this research article.

2. Experimental Program

In this study, five CCI hollow brick masonry walls were constructed and tested under diagonal compression. The details of test matrix are summarized in Table 1. Masonry wall specimens of dimensions 1000×1000×125 mm were constructed from CCI hollow bricks of 250×125×100 mm using running bond pattern as shown in Fig. 1. This size was basically adopted to meet the requirements of lab facilities such as capacity of hydraulic jack, load cell and reaction frame. In the masonry wall specimen W1, the layers of CCI hollow bricks were dry stack without using any mortar or grout as shown in Fig. 2(a). The wall specimens W2-O and W3-N were grouted with OPC - sand grout and HPNSC - sand grout, respectively, Fig. 2(b). The last two walls, i.e., W4-O-R and W5-N-R were also grouted with OPC - sand grout and HPNSC - sand grout, respectively, however, prior to the grout filling, round steel bars of diameter 9 mm were also inserted into the holes of CCI hollow bricks at the end locations and middle as shown in Fig. 3. The masonry wall specimens were named according to the following convention: In wall specimen W4-O-R, W4 is wall number (Number 4), O is representing grout of OPC - sand grout, and last digit R is reinforcement. The CCI hollow brick masonry walls constructed in this experimental program are shown in Fig. 4.

Table 1. Details of experimental program.

Wall name	Binding material	Reinforcement
W1	No	-
W2-O	OPC-sand grout	-
W3-N	HPNSC-sand grout	-
W4-O-R	OPC-sand grout	3RB9
W5-N-R	HPNSC-sand grout	3RB9
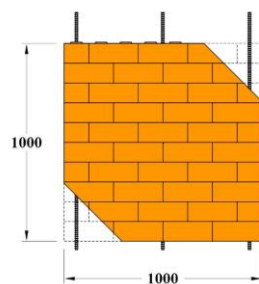
Fig. 1. Typical construction details of masonry walls.

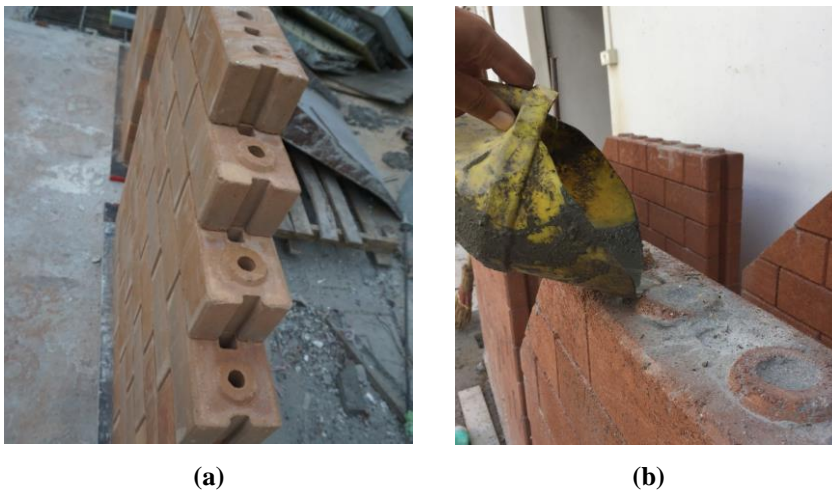(a)   (b)

Fig. 2. Typical constructions of CCI brick masonry walls.
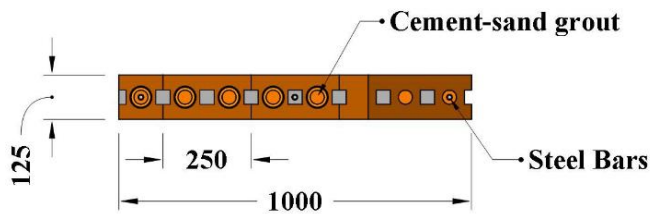

Fig. 3. Details of masonry walls.

Fig. 4. CCI brick masonry walls.

3. Material Properties

In this study, cement stabilized and hydraulically pressed clay interlocking (CCI) hollow bricks were used to construct the masonry walls. The CCI bricks were obtained from the local manufacturer. The brick average gross area and net area were 312.5 cm^2

and 297.7 cm^2, respectively. The CCI hollow bricks are usually manufactured in the following three steps. In the first step, the coarser component materials are broken down into finer material with the help of mechanical grinding machines. These grinding machines are used in sizes ranging from 60 mm to 650 mm and capacities ranging from 40 N/hr to 120,000 N/hr at different manufacturing plants.

In the second step, a concrete mixer machine is used to mix different component materials such as cement, sand, red clay. In the last step, the prepared mix is placed into the aluminium molds and pressed by either hydraulically or manually operated machines [29]. The mix components of the CCI bricks obtained from the manufacture are summarized in Table 2. The compressive strength and water absorption of CCI hollow bricks were obtained by experimental testing according to ASTM C1314-16 standards [31]. Two types of cement grouts i.e., OPC-sand grout and HPNSC-sand grouts were used to fill the holes in the CCI hollow bricks.

OPC and HPNSC were manufactured by Siam Cement Public Company Limited, Thailand and General Engineering Company Limited Thailand, respectively. The cement to sand proportion of 1:2 was used for both types of cement-sand grouts. Cement-sand grout compressive strength was determined by testing 50 mm mortar cube in accordance with ASTM C109/C109M-16a standards [32]. The average compressive strength of OPC-sand grout and HPNSC-sand grout was 25.0 MPa and 50.0 MPa, respectively. Material properties of the steel bars (round bar 9 mm) such as yielding and ultimate tensile strength were determined by testing steel bars in the universal testing machine (capacity of machine = 100 kN) according to the ASTM E8/E8M-16a standards [33]. Three samples of steel bars were tested and the average strength was taken as the representative yield and ultimate strengths. The experimental test results are reported in Table 3.

Table 2. Mix components of the CCI hollow bricks.

Mix Components	Amount (kg/m^3)
Cement	164.0
Red Clay	1636.0
Water	600.0

Table 3. Material properties.

Material properties	CCI hollow bricks	Steel bars (RB9)
Dry density (kg/m^3)	1800.0	
Compressive strength (MPa)	6.74	
Water absorption (kg/m^3)	230.0	
Yielding tensile strength (MPa)	-	340.0
Ultimate tensile strength (MPa)	-	440.0

4. Instrumentation and Loading Setup

In this research, the CCI hollow brick masonry walls were tested under the diagonal compression in the reaction frame having a capacity of 2000 kN. The diagonal compressive load was applied using a hydraulic jack and load intensity was recorded through a calibrated load cell placed under the loading piston of the hydraulic jack. A steel plate (1000×200×20 mm) was placed at the top of the masonry wall to ensure the uniform distribution of the applied load. In addition, a thin layer (thickness = 5 mm) of high strength white cement was also provided at

the top of masonry wall (under the steel plate) to maintain a balance load transfer from steel plate to the masonry wall. The CCI brick walls were instrumented with four linear variable differential transducers (LVDTs) to measure the overall vertical diagonal deformation (L1 and L2), vertical shortening at the mid region (L3) and horizontal extension or lateral dilation of the masonry wall at mid region (L4). During the test, the initiation and propagation of cracks were visually inspected and recorded by photographs. Typical sketches of loading setup and instrumentation details are shown in Fig. 5.
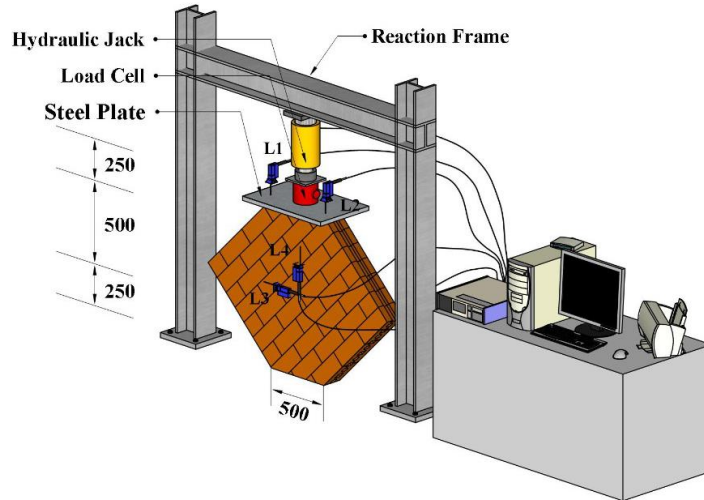

Fig. 5. Loading setup and instrumentation detail (units in mm).

5. Test Results and Discussions

The CCI brick masonry walls were tested in diagonal compression to investigate the efficiency of the selected construction techniques. During the experiment, the load increments and corresponding deformations for both diagonals (i.e., L3 and L4) along with overall diagonal defamation (L1 and L2) were recorded. In this study, the shear strength and shear modulus of the CCI brick wall specimens were calculated using standard equations recommended by ASTM E519/E519M-15 standards [34].

$$S_n = 0.707P/A_n \tag{1}$$

$$\gamma = \Delta V + \Delta H/g \tag{2}$$

$$G = S_n/\gamma \tag{3}$$

where S_n = Shear stress (MPa), P = diagonal compression load (N), A_n = net area of the CCI brick wall specimen (mm^2), w = width of the specimen (mm), h = height of the specimen (mm), t = thickness of the specimen (mm), ΔV = vertical shortening (mm), ΔH = horizontal extension (mm), g = vertical gauge length (mm), G = shear modulus (MPa).

The experimental results in terms of ultimate diagonal compressive load, average diagonal deformation, shear strength (equation 1), and shear modulus

(equation 3) are summarized in Table 4. The experimental responses in terms of diagonal compressive load versus overall average diagonal deformation (average of L1 and L2) curves are graphically shown in Figs. 6 and 7.

Table 4. Experimental results.

Wall name	Load (kN)	Deformation (mm)	% Increase in load	Shear strength (MPa)	Shear modulus (MPa)
W1	27.5	12.5	-	0.62	15.64
W2-O	110.0	1.55	300	2.48	723.44
W3-N	140.0	1.70	409	3.16	468.54
W4-O-R	165.0	2.70	500	3.73	872.19
W5-N-R	180.0	3.00	555	4.07	632.35
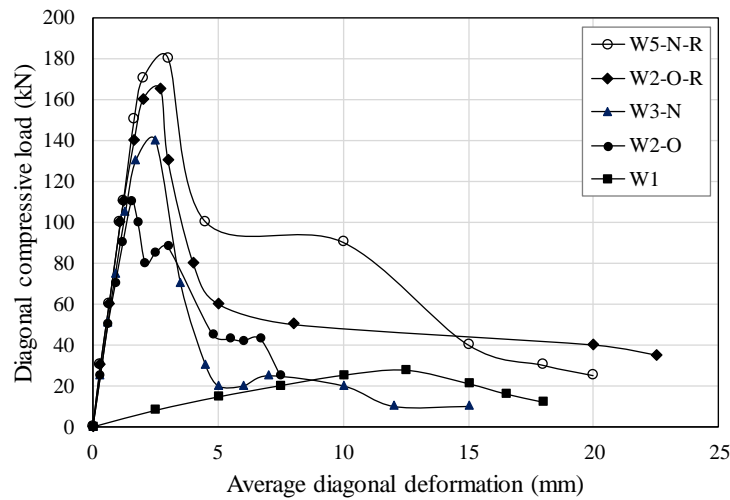
Fig. 6. Diagonal compressive load vs. average diagonal deformation responses.
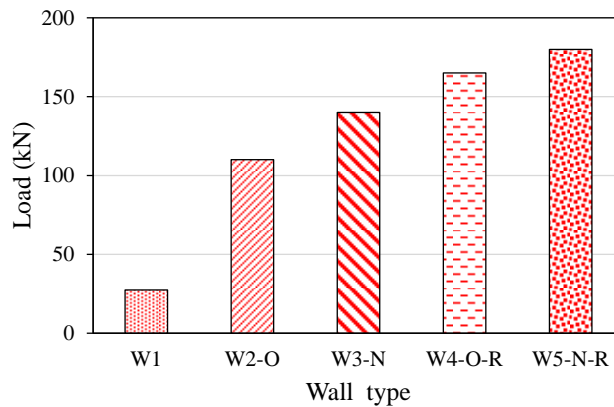
Fig. 7. Ultimate load carrying capacity of walls.

There is a distinct difference between the diagonal compressive load versus overall average diagonal deformation curves of the masonry walls tested in this experimental program both in terms of diagonal compressive load and post peak response. Generally, diagonal compressive load versus diagonal deformation responses of all the tested CCI brick wall specimens were linear up to the ultimate diagonal compressive load. Whereas post peak responses were highly influenced by the presence of cement - sand grout and steel bars. For example, in case of un-grouted CCI brick masonry wall specimen W1, the post peak response indicates a very gradual and linear drop in the diagonal load carrying capacity as shown in Fig. 6. Whereas, post peak response of the of the wall specimen W2-O is indicating a sudden drop in the diagonal load carrying capacity once the ultimate load was reached. However, the post peak response was not observed truly linear. In case of wall specimen W3-N, initially linear post peak response was observed until 80% drop in the load carrying capacity.

In contrast to the un-grouted and unreinforced CCI brick masonry walls, the post peak responses of the reinforced CCI brick masonry walls were found very stable with a slight decrease in the load carrying capacity and large axial deformation as shown in Fig. 6. This phenomenon can be associated with the presence of steel bars. In the reinforced masonry walls, the steel bars provide sufficient resistance to the crack widening, propagation and sudden drop in load. Therefore, the post peak response of the reinforced masonry walls is much stable as compared with un-reinforced masonry walls.

The un-grouted masonry wall specimen (i.e., W1) was failed at the ultimate load of 27.50 kN and average diagonal deformation against the ultimate load was 12.5 mm. The final failure of the wall was mainly due to the sliding of the CCI bricks, splitting and crushing of the CCI hollow bricks. It can be seen (Table 4 and Fig. 6) that the use of both kinds of grouts (i.e., OPC -sand grout and HPNSC-sand grout) is very useful to enhance the diagonal load carrying capacity of the both reinforced and un-reinforced masonry walls. This is because of the reason that the presence of high strength grout increases the bond strength and interlocking strength of CCI hollow brick masonry walls.

The masonry wall specimen (W2-O), in which square and circular holes were filled using OPC -sand grout was reached ultimate load of 110.0 kN, which was 300% higher as compared with the un-grouted CCI hollow brick masonry wall, i.e., W1. The increase in ultimate load was mainly due to the cement grout. In this wall specimen, the diagonal deformation against the ultimate load was recorded as 1.55 mm. The ultimate load carrying capacity and axial deformation of the wall specimen W3-N were observed as 140.0 kN and 1.70 mm, respectively. The load carrying capacity of the wall specimen W3-N was recorded 409% and 109% higher than the wall specimens W1 and W2-O, respectively.

The recorded ultimate load of the wall specimen W3-N was found higher than the wall specimen W2-O (Table 4). This phenomenon can be associated with the high compressive strength of HPNSC-sand grout as compared with OPC-sand grout (see Section 3.0). Previous studies conducted on the diagonal compressive response of masonry walls had also reported that the shear strength of brick masonry walls is highly influenced by the strength of bonding mortar and the compressive strength of the masonry prisms was found higher when using a mortar with high compressive strength as compared with low strength mortar [35-38].

The diagonal ultimate load carrying capacity and diagonal average deformation of the wall specimen W4-O-R were recorded as 165.0 kN and 2.70 mm, respectively. The peak diagonal compressive load was increased by 500% and 200% as compared with wall specimen W1 and W2-O, respectively. The recorded ultimate load of the wall specimen W5-N-R was 180.0 kN and corresponding axial deformation was 3.0 mm. Increases of 555% and 146% in the ultimate diagonal load carrying capacity were observed as compared with wall specimens W1 and W3-N, respectively.

The ultimate load carrying capacity of reinforced masonry walls is found higher than the unreinforced masonry walls, which is mainly due to the presence of steel bars. It is evident from the experimental results that the use of steel bars is very effective to alter both ultimate load carrying capacity and ultimate failure mechanism of the CCI brick masonry walls.

The comparison between the un-grouted and grouted CCI brick masonry walls revels that the use of cement-sand grout and reinforcement increases the shear strength of wall from 2.48 MPa to 3.16 MPa and shear modulus of 468.53 MPa to 723.44 MPa. The comparison between the un-grouted and reinforced CCI brick masonry walls revels that the use of steel bars increases the shear strength of wall from 3.73 MPa to 4.07 MPa and shear modulus from 632.35% to 872.19%.

Only the W1 wall specimens showed lower shear modulus. The higher stiffness and shear strength belongs to reinforced cement sand grouted CCI brick masonry walls. The increase in the shear strength as a result of grouting is in line with findings reported in some previous studies [39] where significant strength increases were observed when comparing fully grouted and hollow specimens.

6. Cracking and Failure Modes of Masonry Walls

In this section, the cracking pattern and failure modes of the tested masonry walls are discussed in detail to investigate the efficiency of cement-sand grout and steel bars to enhance load carrying capacity of CCI brick masonry walls and to alter the cracking modes of CCI brick masonry walls. The load at the first crack stage is referred as cracking load in this study. The cracking loads of the tested masonry walls are summarized in Table 5.

Table 5. Experimental results (cracking load).

Wall name	Cracking load (kN)	% Increase in cracking load
W1	24	-
W2-O	80	233
W3-N	107	346
W4-O-R	84	250
W5-N-R	114	375

6.1. Masonry wall specimen W1

The CCI brick wall specimen, i.e., W1 was constructed without using any binding material and or cement-sand and tested under diagonal compression. In this type of construction, the bond strength is usually achieved through the interlocks of the CCI hollow bricks. In the wall specimen W1, lateral sliding or extension of the CCI

bricks along the both diagonal planes was observed prior to the development of cracks in the wall.

The first visible crack (splitting crack) was observed at the diagonal load of 24 kN under the loading region in the mid location. With the further increase in the load, i.e., at 27 kN, another crack was observed under the loading plate (slightly towards the right side). As the load was increased, i.e., 29 kN, splitting cracks were also noticed at the bottom of the wall, as shown in Fig. 7. As the load was further increased, noticeable sliding of the CCI hollow bricks were observed along the bed joints.

Initiation of the new cracks on the right side was also observed at the diagonal load of 39 kN along with further sliding of the CCI bricks. At this stage, a clear gap of around 1 cm to 2 cm was also noticed between the CCI hollow bricks along the compression diagonal. With the further increase in the load, widening and propagation of the existing cracks along with the crushing of the CCI bricks was noticed. The final failure of the wall specimen W1 was mainly due to the crushing of the CCI bricks (under loading region) and splitting of the CCI bricks (at mid region) as shown in Fig. 8. Based on test observations, the ultimate failure of the wall specimen W1 can be recognized as diagonal tension.

Fig. 8. Failure mode of the wall specimen W1.

6.2. Masonry wall specimen W2-O

In the masonry wall specimen W2-O, the CCI bricks were placed over each other in the running bond pattern (similar to the wall specimen W1), and in the next step, the circular and square holes in the CCI hollow bricks were filled with the OPC - sand grout to enhance the strength and stability of the CCI brick wall masonry, Fig. 2(b). In this case, the first visible crack was noticed at the bottom (right side) of the wall. The recorded cracking load was 80 kN, which was 233% higher than the un-grouted wall specimen W1 (Table 5). This is an indication that use of OPC - sand grout is very effective to delay the damage and to enhance the load carrying capacity of the CCI hollow brick masonry wall. The further increase in load resulted

in a sudden and abrupt crack in the mid region along the full height of compressed diagonal (i.e., from bottom to the loading region).

These cracks were initially observed in the middle region of the compressed diagonal, then propagating abruptly towards loading region and bottom of the CCI brick masonry wall. As the load was further increased, i.e., at 84 kN, splitting of the CCI bricks was also observed at left bottom of the CCI brick masonry wall. The further increase in the load resulted in the widening and propagation of the existing vertical cracks in the middle of the wall. The final failure of the wall specimen W2-O, was mainly due to the splitting of the CCI bricks along the compressed diagonal, sliding of the CCI brick along the bed joint (at bottom region) and crushing of the CCI bricks under loading region and at the bottom of the CCI bricks.

At the ultimate stage, a clear and wide gape (up to 5 cm) was observed at the compressed diagonal as shown in Fig. 9. Previous experimental studies conducted on the diagonal compressive response of block masonry walls [40] have also shown similar kind of failure modes. The ultimate mode of the wall specimen W1 can be recognized as splitting failure.
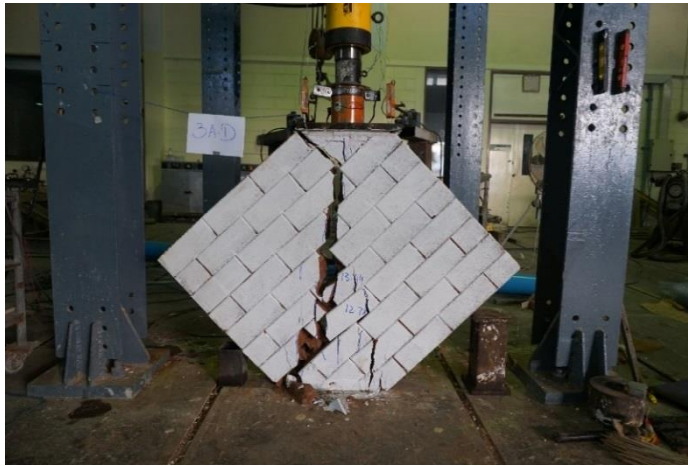

Fig. 9. Failure mode of the wall specimen W2-O.

6.3. Masonry wall specimen W3-N

The construction of the CCI brick masonry wall specimen W3-N was similar to the wall specimen W2-O, except the square and circular holes in the CCI bricks were filled by HPNSC-sand grout instead of OPC - sand grout to enhance the strength and stability of the masonry wall. In this wall specimen, the observed cracking load was 107 kN. The cracking load of the wall specimen W3-N was observed 346% and 113% higher than the wall specimens W1 and W2-O, respectively (Table 5).

This increase in load is an indication that the use of HPNSC-sand grout is very effective to enhance strength and cracking load of the un-grouted masonry walls. It is also evident that use of HPNSC-sand grout is more effective as compared with the OPC - sand grout. This is basically due to the higher strength of the HPNSC-sand grout as compared with the OPC - sand grout (Section 3.0).

In the masonry wall specimen W3-N, the first crack was also developed at the bottom of the masonry wall, following a sudden and abrupt initiation of the vertical crack at compression diagonal similar to the wall specimen W2-O. Few more cracks were also appearing in the middle region at the next loading step i.e., 134 kN. The further increase in the load was resulted in the widening and propagation of the existing cracks along with the development of few more cracks in the lower middle of the wall.

At this stage sliding of the CCI hollow bricks along the bed joints were also observed in the mid of the diagonal compression. The final failure of the wall specimen W3-N, was mainly due to the splitting of the CCI bricks along the compressed diagonal, sliding of the CCI brick along the bed joint (at the bottom region) and crushing of the CCI hollow bricks under loading region and at the bottom of the CCI bricks. Similar to the wall specimen W2-O, a clear and wide gape (up to 5 cm) was observed at the compressed diagonal as shown in Fig. 10. In this wall specimen, large number of splitting cracks were also observed at the bottom of the wall prior to the final failure. The ultimate mode of the wall specimen W3-N can be recognized as splitting failure and diagonal tension failure.

Fig. 10. Failure mode of the wall specimen W3-N.

6.4. Masonry wall specimen W4-O-R

The construction technique of the wall specimen W4-O-R was similar to the CCI hollow brick masonry wall specimen W2-O, however, prior to the OPC-sand grouting, three steel bars (round bars) of diameter 9 mm were also inserted into the holes at different locations as shown in Fig. 3. In this case, the cracking load was recorded as 84 kN and the first crack was noticed at the bottom (left side) of the CCI brick masonry wall.

The cracking load of the wall specimen W4-O-R was observed 250% and 17% higher than the masonry wall specimens W1 and W2-O, respectively, indicating that the use of steel bars is effective to enhance to cracking load of the masonry walls as compared with un-grouted and unreinforced masonry walls. The presence of steel bars is effective to provide resistance to the crack initiation and propagation,

thus resulting in higher load carrying capacity of the masonry walls. Afterward, at a diagonal load of 110-115 kN, several cracks have formed along the compression diagonal strip.

The initial formation of these cracks was similar to the un-reinforced CCI brick masonry walls. However, propagation and widening of these cracks were not sudden and abrupt as compared with un-reinforced masonry walls. Further propagation of these cracks towards the bottom and loading region was observed at the diagonal load of 135-140 kN. This phenomenon (delay in the propagation and widening of the cracks) is a clear indication that use of steel bars is very effective to enhance the diagonal load carrying capacity and to delay the cracking mode of the reinforced CCI hollow brick masonry walls.

Afterword, large lateral dilation and crack widening were observed at the diagonal load of 150-150 kN along with the appearance of several hairline inclined cracks at different locations (mainly at the bottom and under the loading region). The final failure of the wall specimen W4-O-R, was mainly due to the splitting of the CCI bricks along the compressed diagonal, sliding of the CCI brick along the bed joint (under the loading and at bottom region) and crushing of the CCI bricks at different locations along the compression diagonal as shown in Fig. 11.

The final failure of wall specimen W4-O-R was very ductile as compared with the unreinforced masonry walls i.e., W2-O and W3-N. The ultimate failure mode of the wall specimen W4-O-R can be recognized as a combination of shear slip along the bed joints and diagonal tension.

Fig. 11. Failure mode of the wall specimen W4-O-R.

6.5. Masonry wall specimen W5-N-R

The construction of the wall specimen W5-N-R is similar to the masonry wall specimen W3-N, however, prior to the grouting, three round steel bars of diameter 9 mm were also inserted into the holes in the wall ends and middle as shown in Fig. 3. In this case, at first, no crack was noticed at any location, i.e., such as under the

loading region and at bottom of the wall. Then the main crack initiates at compression diagonal similar to the other cement-sand grouted masonry wall specimen and the observed cracking load was 114 kN.

The cracking load of the wall specimen W5-N-R was observed 375% and 29% higher than the masonry wall specimens W1 and W3-N, respectively, indicating that the use of steel bars is effective to enhance the cracking load of the masonry walls as compared with un-grouted and unreinforced masonry walls. The presence of steel bars is effective to provide resistance to the crack initiation and propagation, thus resulting in higher load carrying capacity of the masonry walls. Afterward, propagation of the main crack towards the loading region was observed at diagonal load 116-120 kN.

As the load was further increased, i.e., at 124 kN, the propagation of the main crack was also observed towards the bottom region of the masonry wall. The further increase in the load was resulted in the widening and propagation of the existing cracks along with the development of few more cracks in the lower middle of the wall. Similar to the wall specimen W4-O-R, there was found delay in the crack widening and propagation after the development of initial cracks due to the presence of steel bars. Afterword, large lateral dilation and crack widening were observed at the diagonal load of 150-150 kN along with the appearance of several hairline inclined cracks at different locations (mainly at the bottom location).

The final failure of the wall specimen W5-N-R, was mainly due to the splitting of the CCI bricks along the compressed diagonal, sliding of the CCI brick along the bed joint (at the bottom region) and crushing of the CCI bricks at different locations along the compression diagonal as shown in Fig. 12. The final failure of wall specimen W5-N-R was very ductile as compared with the unreinforced masonry walls i.e., W2-O and W3-N. The ultimate failure mode of the wall specimen W5-N-R can be recognized as a combination of shear slip along the bed joints and diagonal tension.

Fig. 12. Failure mode of the wall specimen W5-N-R.

7. Conclusions

This study presents a comprehensive investigation on the efficiency of cement -sand grouts and steel bars for cement-clay interlocking (CCI) hollow brick masonry walls to enhance the load carrying capacity and to alter the failure modes of the CCI hollow brick masonry walls. An experimental program was established and five CCI hollow brick masonry walls were tested under diagonal compression. Two types of cement sand grouts i.e., OPC - sand grout and HPNSC -sand grout were used along with steel bars. From the conducted tests, the following conclusion can be drawn;

- The un-grouted masonry wall fails in a ductile manner with a large vertical and horizontal deformation.

- The grouted masonry walls (unreinforced masonry walls) in which square and circular holes in the CCI hollow bricks were filled by cement grouts resulted in higher ultimate load carrying capacity, shear strength and shear modulus as compared with un-grouted masonry wall. In general, increasing the grout strength results in increasing the ultimate load carrying capacity of the CCI hollow brick masonry walls. The ultimate failure of the cement-sand grouted masonry walls was observed brittle and sudden.

- In contrast to the unreinforced masonry walls, the overall response of the steel reinforced masonry walls was found significantly improving in terms of diagonal load carrying capacity, shear strength, shear modulus and ultimate failure modes.

- Probably the most obvious suggestion for continued research into CCI hollow brick masonry walls is to the investigate the seismic response of CCI hollow brick masonry walls under lateral loading to simulate the effect of earthquake loading.

Acknowledgement

Nomenclatures	
A_n	Net area of the wall, mm^2
G	Shear modulus, MPa
g	Vertical gauge length, mm
h	Height of the specimen, mm
P	Diagonal compression load, N
S_n	Shear stress, MPa
t	Thickness of the specimen, mm
w	Width of the specimen, mm
Abbreviations	
ASTM	American Society for Testing and Materials
CCI	Cement-Clay Interlocking
ICEBs	Interlocking Compressed Earth Blocks
RB	Round Bars

References

1   Thaickavil, N.N.; and Thomas, J. (2018). Behaviour and strength assessment of masonry prisms. *Case Studies in Construction Materials*, 8, 23-38.

2   Turnšek, V.; and Čačovič, F. (1971). Some experimental results on the strength of brick masonry walls. *Proceedings of the Second International Brick Masonry Conference*. Stoke-on-Trent, United Kingdom, 149-156.

3   Kent, D.C.; and Park, R. (1971). Flexural members with confined concrete. *Journal of the Structural Division*, 97(7), 1969-1990.

4   Calvi, G.M.; and Magenes, G. (1991). Experimental evaluation of seismic strength of old masonry structures. *Proceedings of 9th International Brick/Block Masonry Conference*. Berlin, Gemany, 490-497.

5   Naraine, K.; and Sinha, S. (1989). Behavior of brick masonry under cyclic compressive loading. *Journal of Structural Engineering*, 115(6), 1432-1445.

6   Augenti, N.; and Parisi, F. (2010). Constitutive models for tuff masonry under uniaxial compression. *Journal of Materials in Civil Engineering*, 22(11), 1102-1111.

7   Parisi, F.; and Augenti, N. (2013). Assessment of unreinforced masonry cross sections under eccentric compression accounting for strain softening. *Construction and Building Materials*, 41, 654-664.

8   Li, J.; Masia, M.J.; Stewart, M.G.; and Lawrence, S.J. (2014). Spatial variability and stochastic strength prediction of unreinforced masonry walls in vertical bending. *Engineering Structures*, 59, 787-797.

9   Zavalis, R.; Jonaitis, B.; and Marčiukaitis, G. (2013). Numerical and experimental analysis of grouted hollow block masonry under compression. *Engineering Structures and Technologies*, 5(2), 45-53.

10 Lin, K.; Totoev, Y.Z.; Liu, H.; and Wei, C. (2015). Experimental characteristics of dry stack masonry under compression and shear loading. *Materials*, 8(12), 8731-8744.

11 Faella, C.; Martinelli, E.; Paciello, S.; Camorani, G.; Aiello, M.A.; Micelli, F.; and Nigro, E. (2011). Masonry columns confined by composite materials: Experimental investigation. *Composites Part B: Engineering*, 42(4), 692-704.

12 Mazzotti, C.; Ferracuti, B.; and Bellini, A. (2015). Experimental bond tests on masonry panels strengthened by FRP. *Composites Part B: Engineering*, 80, 223-237.

13 Micelli, F.; Ludovico, M.D.; Balsamo, A.; and Manfredi, G. (2018). Mechanical behaviour of FRP-confined masonry by testing of full-scale columns. *Materials and Structures*, 47(12), 2081-2100.

14 Miccoli, L.; Müller, U.; and Fontana, P. (2014). Mechanical behaviour of earthen materials: a comparison between earth block masonry, rammed earth and cob. *Construction and Building Materials*, 61, 327-339.

15 Gurumo, S.R. (1992). Diagonal compression strength of adobe wall panels. *Master of Engineering Project D Report*. University of Auckland, Auckland, New Zealand.

16 Sathiparan, N.; Mayorca, P.; Nashelli, K.N.; Guragain, R.; and Meguro, K. (2006). Experimental study on unburned brick masonry wallettes retrofitted by pp-band meshes. *Seisan Kenkyu*, 58(3), 301-304.

17   Bartolomé, A.S.; Delgado, E.; and Quiun, D. (2009). Seismic behaviour of a two-story model of confined adobe masonry. *Proceedings of 11ᵗʰ Canadian Masonry Symposium*. Toronto, Ontario, 10 pages.

18   Alecci, V.; Fagone, M.; Rotunno, T.; and De Stefano, M. (2013). Shear strength of brick masonry walls assembled with different types of mortar. *Construction and Building Materials*, 40, 1038-1045.

19   Yardim, Y.; and Lalaj, O. (2016). Shear strengthening of unreinforced masonry wall with different fiber reinforced mortar jacketing. *Construction and Building Materials*, 102(Part 1), 149-154.

20   Nazar, M.E.; and Sinha, S.N. (2006). Influence of bed joint orientation on interlocking grouted stabilized mud-fly ash brick masonry under cyclic compressive loading. *Structural Engineering and Mechanics*, 24(5), 585-599.

21   Nazar, M.E.; and Sinha, S.N. (2007). Behavior of interlocking grouted stabilized sand-fly ash brick masonry under uniaxial cyclic compressive loading. *Journal of Materials in Civil Engineering*, 19(11), 947-956.

22   Ronoh, V.; Too, J.K.; Kaluli, J.W.; and Victor, R.; (2014). Cement effects on the physical properties of expansive clay soil and the compressive strength of compressed interlocking clay blocks. *European International Journal of Science and Technology*, 3(8), 74-82.

23   Laursen, P.T.; Herskedal, N.A.; Jansen, D.C.; and Qu, B. (2015). Out-of-plane structural response of interlocking compressed earth block walls. *Materials and Structures*, 48(1-2), 321-336.

24   Bland, D.W. (2011). *In-plane cyclic shear performance of interlocking compressed earth block walls*. Master Thesis. Faculty of California Polytechnic State University, San Luis Obispo, California.

25   Namboonruang, W.; Rawangkul, R.; Yodsudjai, W.; and Khedari, J. (2011). Investigation of properties of low thermal conductivity pozzolanics soil bricks towards sustainable development. *Advanced Materials Research*, 261-263, 469-479.

26   Namboonruang, W.; Rawangkul, R.; and Yodsudjai, W. (2012). Strength properties of low thermal conductivity fly ash bricks: compressive and flexural strength aspects. *Applied Mechanics and Materials*, 117-119, 1352-1357.

27   Yoosathaporn, S.; Tiangburanatham, P.; and Pathom-aree, W. (2015). The influence of biocalcification on soil-cement interlocking block compressive strength. *Biotechnologie, Agronomie, Société et Environnement*, 19(3), 262-269.

28   Namboonruang, W.; Rawangkul, R.; and Yodsudjai, W. (2013). A perspective study on strength properties-low thermal conductivity and leachability of pozzolanics soil bricks towards to environmentally friendly. *Advanced Science Letters*, 19(10), 2831-2841.

29   Joyklad, P. (2018). Mechanical properties of local cement-clay interlocking bricks in central part of Thailand. *SWU Engineering Journal*, 13(1), 1-12.

30   Shakir, A.A.; and Mohammed, A.A. (2015). Durability property of clay ash, quarry dust and billet scale bricks. *Journal of Engineering Science and Technology* (*JESTEC*), 10(5), 591-605.

31   ASTM International. (2016). Standard test method for compressive strength of masonry prisms. *ASTM C1314-16*.

32   ASTM International (2016). Standard test method for compressive strength of hydraulic cement mortars (using 2-in. or [50-mm] cube specimens). *ASTM C109/C109M-16a*.

33   ASTM International. (2016). Standard test methods for tension testing of metallic materials. *ASTM E8/E8M-16a*.

34   ASTM International. (2015). Standard test method for diagonal tension (shear) in masonry assemblages. *ASTM E519/E519M-15*.

35   Freeda Christy, C.; Tensing, D.; and Mercy Shanthi, R. (2013). Experimental study on axial compressive strength and elastic modulus of the clay and fly ash brick masonry. *Journal of Civil Engineering and Construction Technology*, 4(4), 134-141.

36   Barbosa, C.S.; Lourenço, P.B.; and Hanai, J.B. (2010). On the compressive strength prediction for concrete masonry prisms. *Materials and Structures*, 43(3), 331-344.

37   Khalaf, F.M.; Hendry, A.W.; and Fairbairn, D.R. (1994). Study of the compressive strength of blockwork masonry. *Structural Journal*, 91(4), 367-375.

38   McNary, W.S.; and Abrams, D.P. (1985). Mechanics of masonry in compression. *Journal of Structural Engineering*, 111(4), 857-870.

39   Drysdale, R.G.; and Hamid, A. A. (1979). Behavior of concrete block masonry under axial compression. *American Concrete Institute Journal,* 76(6), 707-721.

40   Kaaki, T. (2013). *Behavior and strength of masonry prisms loaded in compression*. Master Thesis. Dalhousie University Halifax, Halifax, Nova Scotia, Canada.